Scattering of Medium-Energy Alpha Particles. III. Analysis of Elastic and Inelastic Scattering from ^{42}Ca and ^{50}Ti

C. G. MORGAN* AND DAPHNE F. JACKSON

Department of Physics, University of Surrey, Guildford, England

(Received 22 July 1969)

A combined analysis is made of elastic and inelastic scattering of medium-energy α particles from ^{42}Ca and ^{50}Ti. This is first done in terms of the generalized optical model. A conventional distorted-wave Born-approximation inelastic scattering is then made, using phenomenological optical potentials to generate the distorted waves, but using a microscopic description of the nuclear excitation constructed from an effective two-body interaction and shell-model wave functions for the nucleus. Finally, a fully microscopic calculation is made to give a consistent description of the elastic and inelastic scattering, and it is shown that this model is capable of producing results which are comparable, in terms of quality of fit to the data, to those given by the generalized optical model.

1. INTRODUCTION

In two previous papers,[1,2] we have studied the elastic scattering of medium energy α particles using a phenomenological optical potential (Paper I) and a microscopic model for the optical potential (Paper II). We have now extended these calculations to give a combined analysis of elastic and inelastic scattering from two selected nuclei, ^{42}Ca and ^{50}Ti.

We first use the generalized optical model and make a coupled channels analysis of the elastic and inelastic scattering. This allows us to compare the predictions given for inelastic scattering by the various optical potentials obtained in I, and by expressing the nuclear matrix elements in terms of the rotational model, we can extract values for the deformation parameters β_l and the products $\beta_l R_0$ which can be compared with values obtained from other studies of the same nuclei. We then make a DWBA (distorted-wave Born-approximation) analysis of the inelastic scattering using the phenomenological optical potentials to generate the distorted waves, but using a microscopic description of the nuclear excitation in terms of an effective two-body interaction and shell-model wave functions for the nucleus. Finally, we make a fully microscopic calculation to give a consistent description of the elastic and inelastic scattering. This is done in both the DWB and coupled-channel approximations.

For the microscopic calculations, the nuclear wave functions are constructed from the shell-model configurations of the two extra-core nucleons, i.e., two neutrons outside ^{40}Ca and two protons outside ^{48}Ca. It was hoped that this would be a reasonably satisfactory procedure for ^{50}Ti but was not expected to be satisfactory for ^{42}Ca, in which core excitation is known to be important. The second 0^+ and 2^+ states in ^{42}Ca have not been included. The effective interaction for inelastic scattering in DWBA or the coupling potentials for the coupled-channel calculation are then constructed as the matrix elements of the effective two-body (α-nucleon) interaction between the appropriate nuclear states, i.e.,

$$U_{nn'}(\mathbf{R})=\int\rho_{nn'}(\mathbf{r})V_{\text{eff}}(|\mathbf{r}-\mathbf{R}|)d\mathbf{r},$$

where $\rho_{nn'}$ is the transition density

$$\rho_{nn'}(\mathbf{r})=\langle n'|\sum_{1=1}^{A}\delta(\mathbf{r}-\mathbf{r}_i)|n\rangle.$$

V_{eff} is taken to be of Gaussian form, instead of the single Yukawa form used in II, and the parameters are determined by fitting the elastic scattering using the optical potential U_{00}. The ground-state density ρ_{00} and the transition densities are calculated from single-particle wave functions generated in Woods-Saxon potentials. These wave functions have the correct separation energies, as far as these are known, and the proton distributions yield agreement with elastic electron scattering.

2. GENERALIZED OPTICAL MODEL

The coupled-channel calculations were carried out using a computer code based on the one developed by Wills and also using the Atlas library code developed by Hill.[3] These codes gave identical results for the same input data and could be used to describe the coupling of up to three levels. We used the rotational model of Wills,[3] in which the generalized optical potential is expanded in Legendre polynomials. This causes the automatic inclusion of certain higher-order terms in the coupling. However, our purpose in these calculations was not to study the relevance of this model, but rather to compare the predictions, within the framework of

* Present address: Department of Atmospheric Physics, University of Oxford, Oxford, England.

[1] D. F. Jackson and C. G. Morgan, Phys. Rev. **175**, 1402 (1968).

[2] D. F. Jackson and V. K. Kembhavi, Phys. Rev. **178**, 1626 (1969).

[3] J. G. Wills, Ph.D. thesis, University of Washington (unpublished); A. Hill, Atlas Nuclear Physics Programme Library Report (unpublished).

TABLE I. Deformation parameters obtained for ^{42}Ca and ^{50}Ti. Full details of the potential parameters are given in Refs. 1 and 5.

Nucleus	E_{lab} (MeV)	Potential number	V (MeV)	R_0 (F)	β_2	$\beta_2 R_0$ (F)	β_4
^{42}Ca	42	1	47.0	5.55	0.14	0.78	
		4	212.3	4.71	0.18	0.85	0.049
		10	46.1	5.55	0.14	0.78	
		11	112.1	5.06	0.15	0.76	
		12	187.7	4.67	0.17	0.79	
^{50}Ti	44	1	47.6	5.84	0.13	0.76	
		3	196.4	4.99	0.16	0.80	
		4	42.2	5.86	0.14	0.82	
		5	88.5	5.50	0.14	0.74	
		6	207.2	4.98	0.15	0.75	0.067

this model, given by the various optical potentials obtained in I, and to obtain fits to the data which could be compared in terms of quality of fit to those obtained by the microscopic method.

Peterson[4] has measured the cross sections for excitation of the lowest 2^+ state at 1.52 MeV and the 4^+ state at 2.75 MeV in ^{42}Ca at an incident energy of 42 MeV. A variety of parameters for optical potentials of Woods-Saxon form, which had previously been obtained from the analysis[1,5] of the elastic scattering data alone, were used and gave a generally good fit to

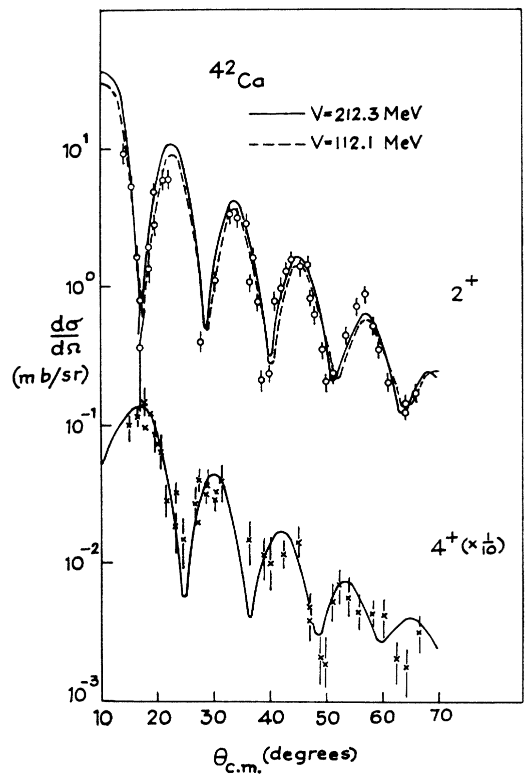

FIG. 1. The cross sections for inelastic scattering from ^{42}Ca at 42 MeV obtained using the generalized optical model. The parameter are given in Table I.

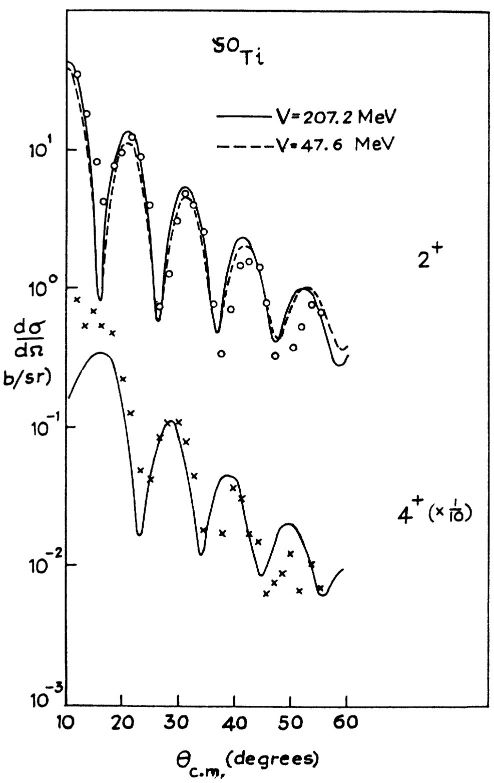

FIG. 2. The cross sections for inelastic scattering from ^{50}Ti at 44 MeV obtained using the generalized optical model. The parameters are given in Table I.

[4] R. J. Peterson, Ph.D. thesis, University of Washington, 1966 (unpublished). More recent measurements indicate that the normalization of Peterson's data may be about 10% low [J. S. Blair (private communication)].

[5] C. G. Morgan, Ph.D. thesis, University of London (unpublished).

TABLE II. Comparison of results for the deformation parameters for ^{42}Ca and ^{50}Ti.

Nucleus	Reference	Reaction	E_{lab} (MeV)	β_2	β_2R_0 (F)	β_4
^{42}Ca	This work	(α, α')	42	0.16	0.79	0.049
	7	$(\alpha, \alpha'$	31	0.19	1.06	0.067
	8	(p, p')	22.9	0.21	0.87	0.105
^{50}Ti	This work	(α, α')	44	0.15	0.78	0.067
	9	(α, α')	43	0.14	0.74	0.073
	10	(α, α')	43	0.15		
	11	(p, p')	17.5	0.15	0.69	0.11
	12	(p, p')	18.2	0.15	0.69	

the data for the 2^+ state. Inclusion of the 4^+ state in the coupled-channel calculation made little difference to the cross section calculated for the 2^+ state. For ^{50}Ti, the cross sections for excitation of the 2^+ and 4^+ states at 1.57 and 2.75 MeV, respectively, have been measured by Bruge *et al.*[6] at an incident energy of 44 MeV. In this case also, the inclusion of the 4^+ state had little effect on the cross sections of the 2^+ state. Typical results for the cross sections are shown in Figs. 1 and 2, and the values of β_2, β_4, and β_2R_0 are given in Table I.

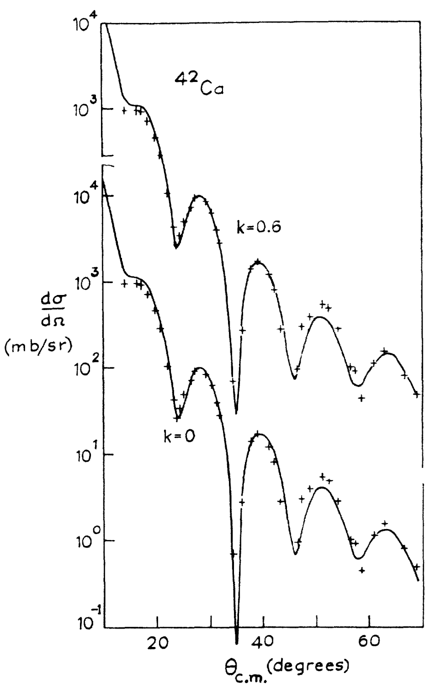

FIG. 3. The cross section for elastic scattering from ^{42}Ca at 42 MeV obtained using the microscopic model. The parameters are given in Table III for the density-independent potential ($k=0$) and in Table IV for the density-dependent interaction ($k\neq 0$).

[6] G. Bruge, Saclay Report No. CEA-R 3147, 1957 (unpublished).

It can be seen from Table I that the different optical potentials produce consistent results for β_2 and β_2R_0. (The parameter β_4 has been determined for only one potential in each case, because of the length of time required for the computation.) In Table II,[7–12] we give the values of these parameters found in DWBA analy-

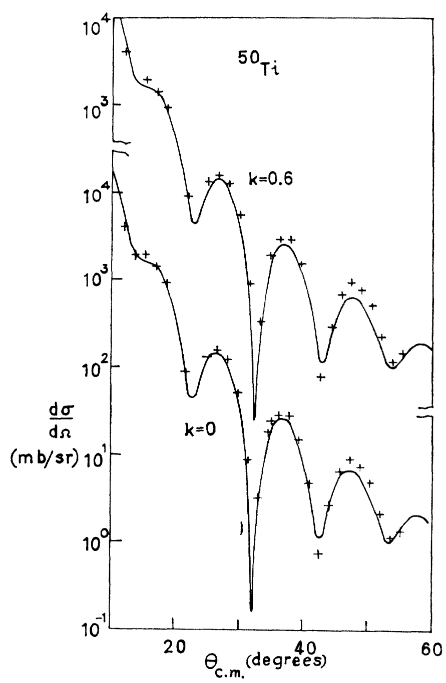

FIG. 4. The cross section for elastic scattering from ^{50}Ti at 44 MeV obtained using the microscopic model. The parameters are given in Table III.

[7] E. P. Lippencott and A. M. Bernstein, Phys. Rev. **163**, 1170 (1967).
[8] J. S. Bane, J. J. Kraushaar, B. W. Ridley, and M. M. Stautberg, Nucl. Phys. **A116**, 580 (1968).
[9] J. L. Yntema and G. R. Satchler, Phys. Rev. **161**, 1137 (1967).
[10] G. R. Satchler, J. L. Yntema, and H. W. Brock, Phys. Letters **12**, 55 (1964).
[11] H. O. Funsten, N. R. Robertson, and E. Rost, Phys. Rev. **134**, B117 (1964).
[12] W. S. Gray, R. A. Kenefick, and J. J. Kraushaar, Nucl. Phys. **67**, 565 (1965).

TABLE III. Results obtained for elastic scattering using the calculated potentials with parameters $K=0.5\ \mathrm{F}^{-1}$ and a density-independent interaction.

	E_{lab} (MeV)	V_0 (MeV)	W_0 (MeV)	$R_{1/2}$ (F)	$V(R_{1/2})$ (MeV)	$W(R_{1/2})$ (MeV)	χ^2
^{42}Ca	42	35.6	13.4	7.33	−2.30	−0.87	8.4
^{50}Ti	44	36.3	11.8	7.61	−2.50	−0.60	3.8

ses of other data for the same nuclei, and from these it appears that our results at 42–44 MeV are in satisfactory agreement with all other analyses.

3. ELASTIC SCATTERING IN THE MICROSCOPIC MODEL

In this work, the α-nucleon interaction is taken to be of Gaussian form, i.e.,

$$V_{\mathrm{eff}}(\mathbf{r}-\mathbf{R})=-V_0\exp[-K^2(\mathbf{r}-\mathbf{R})^2].$$

A preliminary estimate of the parameters V_0 and K was obtained by requiring that the calculated optical potential has the same shape as the phenomenological optical potential in the important surface region. This gave[13] $V_0\approx 50$ MeV, $K=0.5\ \mathrm{F}^{-1}$. It was also found that, in the surface region, variations in K changed the magnitude of the potential but had little effect on the shape. For this reason, the parameter K was fixed at $0.5\ \mathrm{F}^{-1}$. The calculated potential $U_{00}(R)$ was then used in an ordinary optical-model search code. The imaginary part of the potential was taken to have the same radial behavior, and strength determined by an additional parameter W_0. The search code then determined the values of the two parameters V_0 and W_0 which yield a best fit to each set of elastic scattering data. The calculated cross sections are compared with the data in Figs. 3 and 4, and the relevant parameters are given in Table III. Comparison with the results given in I shows that the quality of fit is comparable to that obtained using a phenomenological potential with many more parameters. The values of the strong absorption radii $R_{1/2}$ and the magnitudes of the real and imaginary parts of the potential at the strong absorption radii, $V(R_{1/2})$ and $W(R_{1/2})$, are identical to those obtained in I.

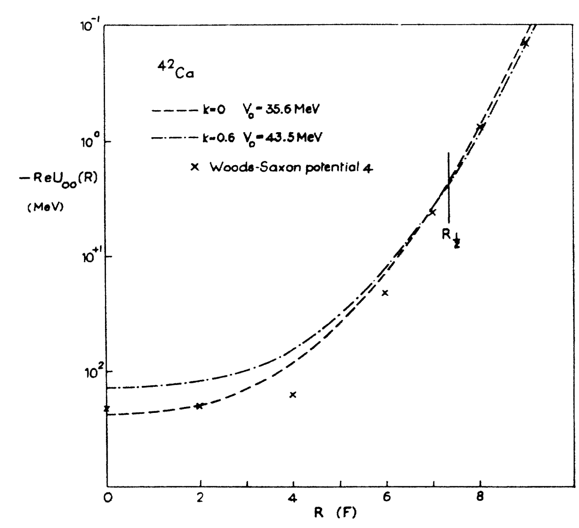

FIG. 5. The optical potentials for ^{42}Ca calculated from the microscopic model, and used to generate the cross sections shown in Fig. 3.

The optical potential has also been calculated with a density-dependent interaction using the expression

$$U_{00}(\mathbf{R})=\int\rho_{00}(r)\,V_{\mathrm{eff}}(\mathbf{r}-\mathbf{R})[1-k\rho_{00}(r)g\rho_{00}(0)]d\mathbf{r},$$

where $\rho_{00}(r)$ is the nuclear density in the ground state, and V_{eff} is still of Gaussian form. The effect of varying the parameter k between zero and unity is to reduce the contribution from the inner region of the nucleus. However, in order to fit the data the parameters V_0, W_0 must be increased as k is increased so that the potential remains the same in the surface region, as can be seen from the potentials shown in Fig. 5 and the results are given in Table IV. Some fits to the data with $k\neq 0$ are shown in Figs. 3 and 4. Comparison of these results with those obtained in II using a Yukawa interaction confirms the conclusion reached in II that the choice of V_{eff} is of crucial importance for a satisfactory fit to the data. The Gaussian interaction used here is is sufficiently sharply peaked so that it produces an optical potential with the required behavior in the surface region, whereas the Yukawa interaction produced a potential which was too diffuse and hence did not reproduce the pronounced diffraction minima of

TABLE IV. Parameters of the optical potentials for ^{42}Ca at 42 MeV.

k	V_0 (MeV)	W_0 (MeV)	χ^2
0	35.6	13.4	8.4
0.2	37.3	14.5	7.8
0.4	43.4	17.9	10.1
0.6	43.5	18.1	9.0
0.8	44.4	18.8	7.8

[13] D. F. Jackson, Nucl. Phys. A123, 273 (1969).

TABLE V. Two-body potential strengths required for the microscopic DWBA calculation with phenomenological optical potentials. The potential numbers refer to the optical potentials which are the same as those listed in Table I.

Nucleus	E_{lab} (MeV)	Potential number	V (MeV)	V_0 (MeV) 2^+ state	V_0 (MeV) 4^+ state
^{42}Ca	42	10	46.1	120	100
		11	112.1	160	100
		12	187.7	150	100
^{50}Ti	44	4	42.2	210	210
		5	87.1	220	220
		6	207.2	205	200

the elastic scattering data. By folding a Gaussian nucleon-nucleon potential into the nuclear density of the α particle, Bernstein[14] has derived a Gaussian α-nucleon potential with parameters V_0 and K which are very close to those determined in this analysis. It is encouraging that there is reasonable agreement between the two sets of parameters, since this suggests that there is internal consistency in the microscopic description, but close agreement is probably fortuitous in view of the number of approximations made in both calculations.

4. INELASTIC SCATTERING IN THE MICROSCOPIC MODEL

The Gaussian α-nucleon interaction was also used to construct the effective interaction for excitation of low-lying states in ^{42}Ca and ^{50}Ti. It was found that the effect of configuration mixing of the two extra-core nucleons is negligible, and so the nuclear wave functions were constructed from the $(1f_{7/2})^2$ configuration. Figure 6 shows the behavior of the radial parts, or form factors, of the effective interactions for the excitation of the 2^+, 4^+, and 6^+ states in ^{42}Ca. The magnitude of the effective interactions should be fixed by the strength V_0 of the α-nucleon potential which has been determined from the analysis of the elastic scattering data described in Sec. 3. We preferred, however, to treat V_0 as a free parameter in the inelastic scattering and then to use the comparison of the values of V_0 required as a test of the microscopic model.

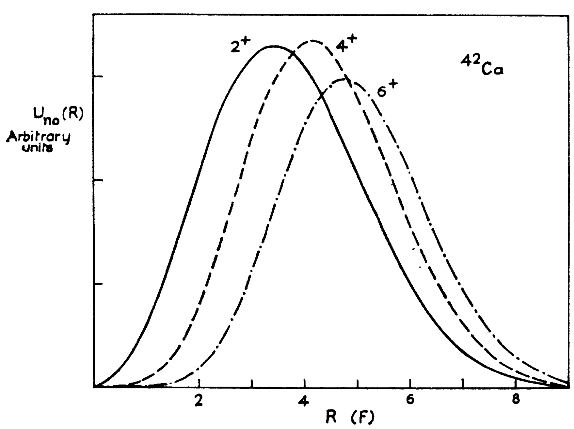

FIG. 6. The form factors of the effective interaction for the excitation of the lowest 2^+, 4^+, and 6^+ states in ^{42}Ca calculated from the microscopic model.

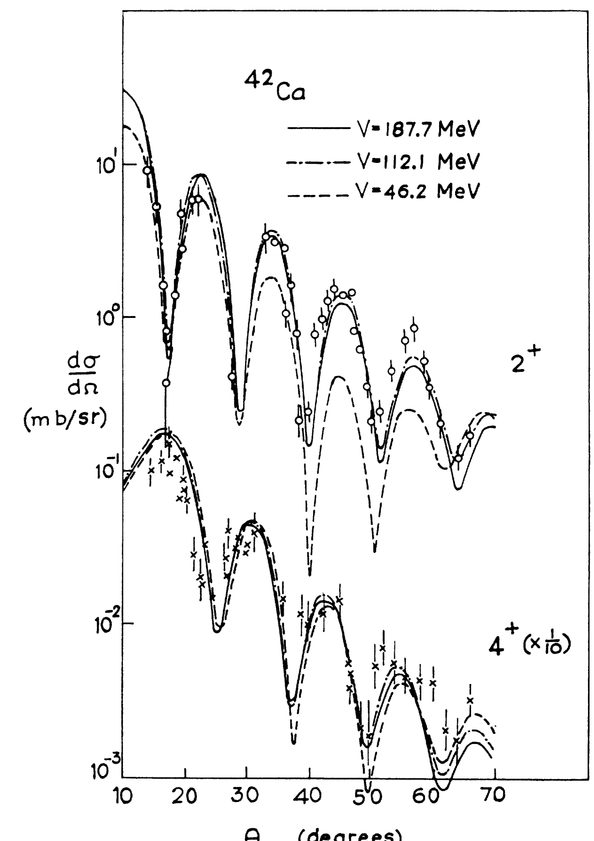

FIG. 7. The cross sections for inelastic scattering from ^{42}Ca at 42 MeV obtained using the microscopic model in DWBA with phenomenological distorting potentials. The parameters are given in Table V.

[14] A. M. Bernstein, Advan. Nucl. Phys. 3 (to be published).

TABLE VI. Two-body potentials strengths required for the fully microscopic calculation. The values quoted for the 0^+ ground state are those obtained from elastic scattering and listed in Table III.

Nucleus	E_{lab} (MeV)	k	V_0 (MeV) 0^+ state	V_0 (MeV) 2^+ state	V_0 (MeV) 4^+ state	V_0 (MeV) 6^+ state	Method
^{42}Ca	42	0	35.6	140	90	~140	DWBA
		0	35.6	140	90		Coupled channel
^{50}Ti	44	0	36.3	190	190		DWBA
		0	36.3	190	190		Coupled channel
		0.6	42.5	190	190		Coupled channel

In the first set of DWBA calculations, the distorted waves were generated in the phenomenological optical potentials of Woods-Saxon form which were previously used in the calculations with the generalized optical model described in Sec. 2. For ^{42}Ca at 42 MeV, the two deeper optical potentials used gave good fits to the inelastic cross section for the 2^+ state, as can be seen from Fig. 7, but the shallow potential gave a very poor fit. All three potentials gave good fits to the inelastic cross section for the 4^+ state, but the values of V_0 required to fit the magnitude of this cross section differ from the values required to fit the 2^+ state or the elastic scattering. These values are given in Table V. For ^{50}Ti at 44 MeV, the deep potential again gives a good fit to the 2^+ cross section, while the shallow potential gives a poor fit, as can be seen from Fig. 8. The intermediate and the deepest potential both yield reasonable fits to the 4^+ cross section, and in this case the same value of V_0 is required for the 2^+ and 4^+ states.

Finally, the full microscopic model was used for both DWBA and coupled-channel calculations. In the latter, the diagonal coupling potentials were calculated using

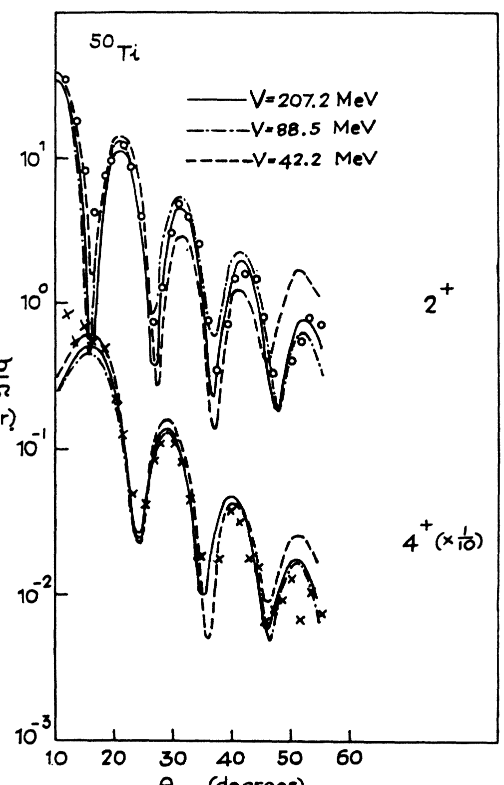

FIG. 8. The cross section for inelastic scattering from ^{50}Ti at 44 MeV obtained using the microscopic model in DWBA with phenomenological distorting potentials. The parameters are given in Table V.

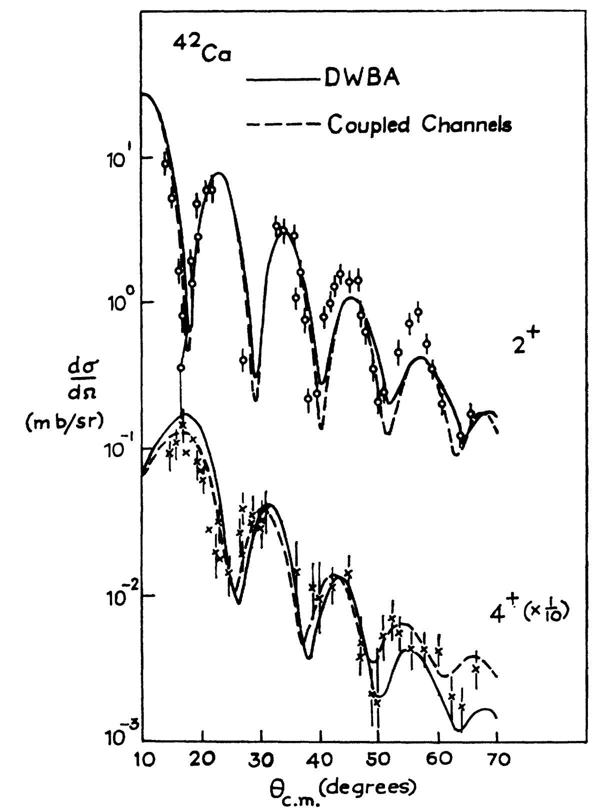

FIG. 9. The cross sections for inelastic scattering from ^{42}Ca at 42 MeV obtained using the full microscopic model. The parameters are given in Table VI.

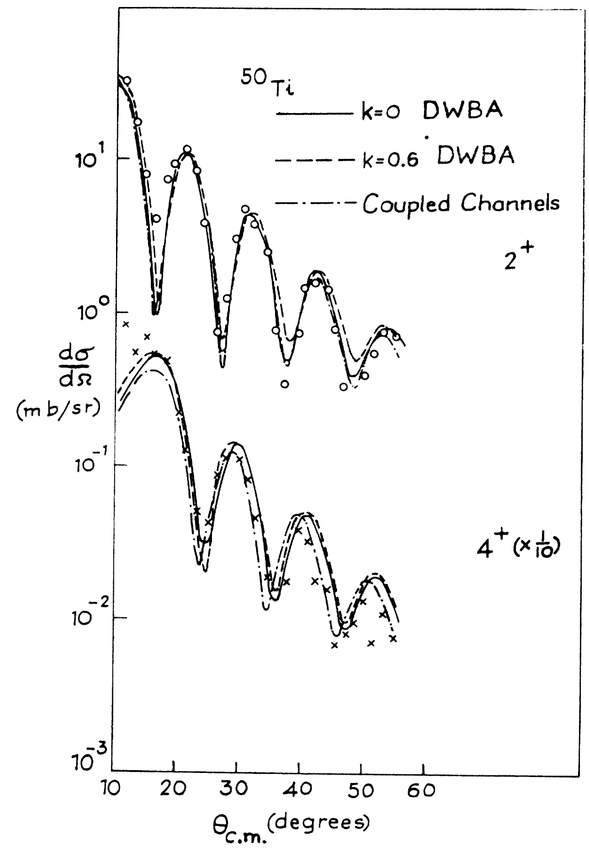

FIG. 10. The cross sections for inelastic scattering from ^{50}Ti at 44 MeV obtained using the full microscopic model. The parameters are given in Table VI.

the effective α-nucleon interaction obtained by fitting the elastic scattering data, but the strength of the α-nucleon interaction used to calculate the off-diagonal terms was allowed to vary. In a coupled-channel calculation with two levels included, this procedure leads to two different values of V_0 which are associated in Table VI with the 0^+ and 2^+ states for ease of comparison with the DWBA results. When three levels are included, the same procedure is followed and the strength V_0 used for the diagonal terms is associated with the 2^+ state. In the case of the three-level calculation for ^{42}Ca, it was necessary to renormalize the predicted 4^+ cross section to bring it into agreement with the data and the DWBA calculation; the product of the renormalization factor and the strength V_0 has been given in Table VI as the strength V_0 for the 4^+ state. In all cases, the coupling potentials are real.

For ^{42}Ca at 42 MeV, the DWBA calculations yield fits to the 2^+ and 4^+ cross sections which are quite comparable with those obtained in Sec. 2, as can be seen from Fig. 9, but the fit to the 6^+ cross section is poor. The values of V_0 required are in agreement with those required in the previous DWBA analysis with the deep optical potential but are, unfortunately, not constant for all the levels considered. The two-level coupled-channel calculation yields almost identical results to the DWBA calculation; there is a slight change in the results obtained when three levels are included, and it is necessary to renormalize the 4^+ cross section to obtain a magnitude fit to the data. For ^{50}Ti at 44 MeV, the DWBA and coupled-channel calculations yield good fits to the data, as shown in Fig. 10, and the value of V_0 used for the off-diagonal potentials is constant, as it should be. One coupled-channel calculation was made with the density-dependent effective interaction described in Sec. 3, and it was found that the qualtity of fit and the values of V_0 required were comparable with the other calculations.

5. DISCUSSION

We conclude from these results that the full microscopic model is capable of producing cross sections for elastic and inelastic scattering of medium-energy α particles which are comparable in terms of quality of fit to those produced by the generalized optical model. When the microscopic model is used for inelastic scattering only, by far the best results are obtained when the deep optical potentials with $V\approx 200$ MeV are used. Since these deep potentials correspond closely to the potentials calculated from the microscopic model, we take this as evidence in support of our earlier arguments[2,15] that the treatment of elastic and inelastic scattering should be consistent.

The description we have given for the two nuclei ^{42}Ca and ^{50}Ti in terms of the shell model without core excitation is evidently inadequate and this has shown up in the variations of the α-nucleon strength parameters listed in Tables V and VI. It is reassuring, however, that these parameters show a more uniform behavior for ^{50}Ti, where we expect the nuclear model to be less defective, than for ^{42}Ca. Within the framework of this nuclear model, the effect of coupling is rather small, so that any uncertainties in our treatment of the coupling should not affect the general conclusions.

ACKNOWLEDGMENT

We gratefully acknowledge encouragement and criticism from Professor J. S. Blair.

[15] D. F. Jackson, Phys. Letters 14, 118 (1964).